Sub-nanometer resolution over several microns range with real-time dual-wavelength digital holographic microscopy

Jonas Kühn[a], Tristan Colomb[b], Christophe Pache[a], Florian Charrière[a] and Christian Depeursinge[a]

[a]*Ecole polytechnique fédérale de Lausanne (EPFL), Institute of imaging and applied optics, CH-1015 Lausanne, Switzerland*

[b]*Centre de Neurosciences Psychiatriques, Département de psychiatrie DP-CHUV, Site de Cery, 1008 Prilly- Lausanne, Switzerland*

Abstract: Single-acquisition dual-wavelength digital holographic microscopy provides real-time phase measurement range over several microns. We demonstrate axial resolution enhancement down to sub-nanometer range thanks to the non-correlation between both available wavefronts.

OCIS codes: (090.1995) Digital holography; (110.0180) Microscopy

1. Introduction

Digital holographic microscopy (DHM) enables to reconstruct the complex wavefront diffracted by an object, both in amplitude and noticeably in phase [1–4]. The interferometric nature of the method enables to reach nanometer-range axial resolution without any scanning procedures, while the lateral resolution remains diffraction-limited, proportional to the numerical aperture (NA) of the microscope objective (MO). The use of digital cameras for hologram recording combined with nowadays high-performance computers allows for video-rate reconstructions in real-time, otherwise camera speed-limited with postponed processing.

However, the phase information is intrinsically only defined modulo 2π, as optical path lengths (OPL) larger than one time the wavelength cannot be unequivocally measured, resulting in a so-called phase ambiguity and presence of phase jumps (wrapped phase). In a lot of situations phase unwrapping algorithms can be applied to retrieve the true OPL map of the sample, but high aspect-ratio objects, as well as noisy experimental conditions, result in the failing of such algorithms.

A classical solution to this single-wavelength phase ambiguity is to combine two wavelengths to obtain a so-called beat-wavelength phase map, where the beat-frequency is equal to the frequency difference. This has been already used intensively in digital holography [5–8] but all theses methods require a sequential approach to record the interferograms from both sources. Consequently real-time dual-wavelength measurements are not possible because at least two camera acquisitions are needed, which is a strong limitation for e.g. monitoring moving samples or measuring in presence of vibrations.

Recently, we proposed a multi-reference waves DHM configuration as a solution to overcome these drawbacks, with a dual-wavelength spatial multiplexing technique enabling single-acquisition beat-wavelength measurements, thus maintaining the real-time capability of DHM [9]. Despite the important improvement over existing techniques, in this work the topographic noise level is increased proportionally with the beat-wavelength, although so-called dual-wavelength unwrapping methods could be used to recover nanometer-precision as in Refs. [6, 7].

Here we show that not only the axial resolution can be conserved as with single-wavelength DHM over several microns, but that it can be furthermore improved down to nearly sub-nanometer regimes by a wavefront spatial averaging, taking advantage of the simultaneous availability of two uncorrelated wavefronts within the same acquisition window.

2. Single-acquisition dual-wavelength digital holography with nanometer resolution

The optical configuration used for dual-wavelength DHM is the one of Ref. [9], with orthogonal reference waves for the two different wavelengths interfering with collinear object waves on the CCD camera as illustrated in Fig. 1(a). It results in an incoherent addition of both wavelengths interferograms and a spatial multiplexing of the hologram permitting separate spatial filtering of the wavefronts in the Fourier domain (see Fig. 1(b,c)).

Once each wavefront (usually the virtual images $\mathbf{R}_1^*\mathbf{O}_1$ and $\mathbf{R}_2^*\mathbf{O}_2$) is separately filtered in the Fourier domain according to Fig. 1(c), they can both be digitally propagated in parallel in the convolution formalism (see Ref. [9]) to

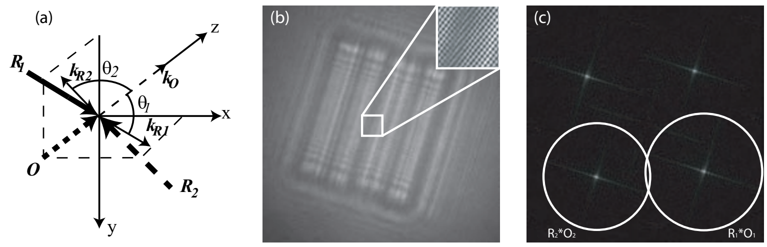

Fig. 1. (a) Geometrical configuration of the beams impeding on the CCD camera: $\mathbf{R}_1$, reference wave for first wavelength λ_1; $\mathbf{R}_2$, reference wave for second wavelength λ_2;**O** superposed object waves for both wavelength parallel to the optical axis; (b) Dual-wavelength hologram where the two interference regimes are clearly visible in the zoomed inset; (c) Fourier-spectrum of (b) where each wavefront can easily be spatially filtered in a separate manner

the image plane, possibly with different reconstruction distances in case of chromatic aberrations. Then computing the difference between both phase map yields the so-called beat-wavelength phase map, as exhibited in Eq.1.

$$\Phi = \arg\left(\boldsymbol{O}_1\boldsymbol{O}_2^*\right) = \phi_1 - \phi_2 = 2\pi\frac{x}{\lambda_1} - 2\pi\frac{x}{\lambda_2} = 2\pi x\left(\frac{\lambda_2-\lambda_1}{\lambda_1\lambda_2}\right) = 2\pi\frac{x}{\Lambda}, \tag{1}$$

where x is the OPL (twice the topography in reflection, for an homogeneous sample in air), ϕ_i the reconstructed phase for the wavelength λ_i and Λ is the synthetic beat wavelength defined as:

$$\Lambda = \frac{\lambda_1\lambda_2}{\lambda_2-\lambda_1}. \tag{2}$$

Typically Λ can reach several microns or more depending on the wavelength difference as can be seen in Eq.2, extending the topographic measurement range without phase ambiguity to $\Lambda/2$. However, despite this advantage, the synthetic phase Φ is affected by an amplification of the phase noise on ϕ_1 and ϕ_2 by a factor Λ/λ_i, meaning that the increased dynamic range is downgraded by a loss of axial resolution. Nevertheless, it is well known that under reasonable noise levels and sufficiently small beat-wavelength values, the synthetic phase map can be used to recover the integer multiple of the wavelength to unwrap or solve the phase ambiguity of one of the single-wavelength phases [6,7]. Practically one compute a new phase map as given by the expression in Eq. 3.

$$\phi_{i,unwrapped} = 2\pi E\left(\frac{\Phi}{2\pi\lambda_i}\right) + \phi_i \tag{3}$$

where $E(x)$ is an integer division.

In addition to this, we propose here an additional increase of resolution compared to single-wavelength DHM by computing the spatial average between both $\phi_{1,unwrapped}$ and $\phi_{2,unwrapped}$. Indeed, these two phase maps correspond to two different wavefronts which are uncorrelated, as they are generated by different laser sources of different wavelengths. Assuming Gaussian phase noise, one can expect that a theoretical topographic resolution improvement factor of $\sqrt{2}/2$ is achievable by a wavefront averaging (variance of a sum).

3. Results

Figure 2 presents results obtained on a up to 1.275 μm high gold-coated Si staircase sample with two laser sources of wavelength λ_1 = 680 nm and λ_2 = 760 nm, yielding Λ = 6.4 μm for the synthetic beat wavelength. It shows clearly that the single-wavelength precision can be conserved over the entire 3.2 μm measurement range. Indeed, with this configuration the noise level on both ϕ_1 and ϕ_2 is below 4°, which is good enough to avoid faulty integer division in Eq. 3 for a synthetic wavelength Λ = 6.4 μm.

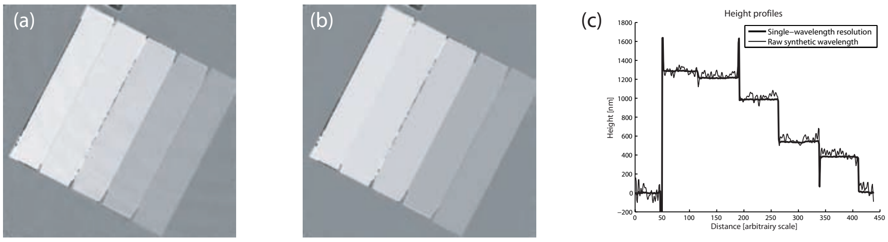

Fig. 2. (a) Raw beat-wavelength topographic map at Λ = 6.4 μm obtained according to Eq. 1; (b) High-resolution averaged topographic map between λ_1 = 680 nm and λ_2 = 760 nm maps unwrapped with (b) according to Eq. 3; (c) Profiles comparison taken along the sample on (b) and (c), where the low-resolution beat-wavelength topographic map is clearly improved when using the expression of Eq. 3 to solve the phase ambiguity only, while keeping the single-wavelength precision

To demonstrate sub-nanometer precision along the optical axis we used the same setup to investigate a 8.5 nm high calibrated step sample, now with λ_1 = 657 nm and λ_2 = 680 nm. The resulting topographic profiles and spatial standard deviations are presented in Fig. 3, which verify the hypothesis of uncorrelated Gaussian noise. Consequently, roughly 30% improvement can be achieved by combining both wavefronts information, thus breaking the nanometer barrier.

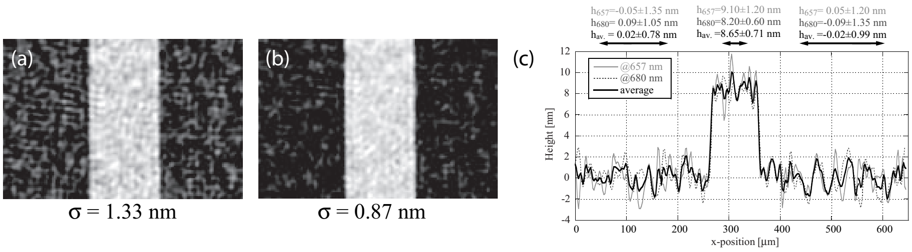

Fig. 3. (a) Topographic map of the 8 nm step at λ_1 = 657 nm, with the corresponding spatial standard deviation over the flat surfaces; (b) Spatially averaged topographic map of both λ_1 = 657 nm and λ_2 = 680 nm maps, with a sub-nanometer standard deviation and an obvious "granularity" reduction on the image; (c) Transverse profiles comparison across the sample, for respectively λ_1 = 657 nm, λ_2 = 680 nm and the spatial average of both, where sub-nanometer resolution is achieved

4. Conclusion

We presented advanced dual-wavelength digital holographic microscopy results, with unprecedent advantages. First, real-time imaging is possible thanks to the single-acquisition procedure. Moreover, we demonstrated that not only the single-wavelength precision can be kept throughout the extended measurement range, but that the resolution can be even increased down to sub-nanometer regimes by making advantage of the two uncorrelated wavefronts simultaneously available. This is promising to achieve more than 3 decades dynamic range for DHM measurements.

References

1. J. W. Goodman and R. W. Lawrence, “Digital image formation from electronically detected holograms,” Applied Physics Letters **11**, 77–79 (1967).
2. U. Schnars and W. Jüptner, “Direct Recording of Holograms by a Ccd Target and Numerical Reconstruction,” Applied Optics **33**, 179–181 (1994).
3. E. Cuche, F. Bevilacqua, and C. Depeursinge, “Digital holography for quantitative phase-contrast imaging,” Optics Letters **24**, 291–293 (1999).
4. E. Cuche, P. Marquet, and C. Depeursinge, “Simultaneous amplitude-contrast and quantitative phase-contrast microscopy by numerical reconstruction of Fresnel off-axis holograms,” Applied Optics **38**, 6994–7001 (1999).
5. C. Wagner, W. Osten, and S. Seebacher, “Direct shape measurement by digital wavefront reconstruction and multiwavelength contouring,” Optical Engineering **39**, 79–85 (2000).
6. J. Gass, A. Dakoff, and M. K. Kim, “Phase imaging without 2 pi ambiguity by multiwavelength digital holography,” Optics Letters **28**, 1141–1143 (2003).
7. D. Parshall and M. Kim, “Digital holographic microscopy with dual wavelength phase unwrapping,” Applied Optics **45**, 451–459 (2006).
8. I. Yamaguchi, T. Ida, M. Yokota, and K. Yamashita, “Surface shape measurement by phase-shifting digital holography with wavelength shift,” Applied Optics **45**, 7610–7616 (2006).
9. J. Kühn, T. Colomb, F. Montfort, F. Charrière, Y. Emery, E. Cuche, P. Marquet, and C. Depeursinge, “Real-time dual-wavelength digital holographic microscopy with a single hologram acquisition,” Optics Express **15**, 7231–7242 (2007).